

Quantum computation with doped silicon cavities

M. Abanto,^{1,*} L. Davidovich,¹ Belita Koiller,¹ and R. L. de Matos Filho¹

¹*Instituto de Física, Universidade Federal do Rio de Janeiro,
Caixa Postal 68528, Rio de Janeiro, RJ 21941-972, Brazil*

(Dated: February 21, 2024)

We propose a quantum computer architecture involving substitutional donors in photonic-crystal silicon cavities and the optical initialization, manipulation, and detection processes already demonstrated in ion traps and other atomic systems. Our scheme considerably simplifies the implementation of the building blocks for the successful operation of silicon-based solid-state quantum computers, including positioning of the donors, realization of one- and two-qubit gates, initialization and readout of the qubits. Detailed consideration of the processes involved, using state-of-the-art values for the relevant parameters, indicates that this architecture might lead to errors per gate compatible with scalable quantum computation.

PACS numbers: 03.67.Lx, 71.55.Cn, 42.50.Pq

The search for a working quantum computer has comprised areas ranging from optics to atomic and condensed-matter physics [1]. Finding physical systems that allow for accurate operations has been a formidable challenge, yet to be met. Indeed, the viability of quantum computers depends on finding physical systems that allow scalable fault-tolerant computation, which means that the errors remain bounded when the number of qubits increases. In order to have scalable quantum computation, the error per gate (EPG) should be smaller than a certain threshold, which depends on the specific error-correction scheme. For independent and identically distributed errors, the best lower bound so far is 1.9×10^{-4} [2]. For other architectures, which require however a large resource overhead [3], this threshold is bounded below by 1.04×10^{-3} [4].

Semiconductor devices [5, 6], and most particularly those based on silicon [7], have attracted considerable attention, but actual realization is hindered by difficulties concerning scalability, detection and fabrication [8]. Most candidates for a semiconductor-based quantum computer rely on spin-1/2 fermion qubits [9], which for Si may be associated to the long-lived electron and nuclear spins of shallow substitutional donors [7]. In fact, electronic spin decoherence times have been shown to be larger than 60 ms in ^{28}Si (isotopically purified) at temperatures of 7 K [10]. Implementation of quantum computation with these systems is hindered by several problems. The most obvious [8] is the difficulty in the manipulation and measurement of single-spin states. Two-qubit operations relying on exchange gates [5], restricted to nearest-neighbor interactions, have limited scalability potential [11]. The particular electronic band structure of bulk Si leads to fast oscillations in the electronic exchange coupling when the interacting donor-pair relative position is changed on a lattice-parameter scale [12]. Thus, proposals based on this mechanism require nanofabrication techniques far beyond current capabilities.

Here we propose placing the donors in a single-mode

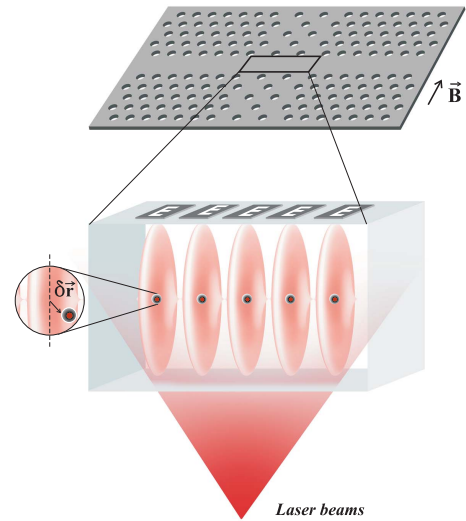


FIG. 1: Proposed quantum-computer architecture. Donor impurities are placed in the neighborhood of intensity maxima of a photonic crystal cavity mode, not necessarily every maximum. The donors are under the action of a uniform magnetic field \vec{B} and electric fields \vec{E} , produced by the electrodes E . The magnetic field is strong enough to decouple nuclear and electronic spins in the donor ground state, and Zeeman-splits two electronic spin states, $|\uparrow\rangle$ and $|\downarrow\rangle$, which constitute the qubit. Turning on the electric fields allows to switch off individual qubit Raman transitions induced by the two laser beams, spread out over the ensemble of qubits, and also the coupling among different qubits through the vacuum cavity field. The inset displays the misplacement $\delta \vec{r}$ of an impurity from a maximum of the cavity mode.

photonic-crystal Si cavity [13], and optically addressing them through Raman transitions induced by the cavity mode and only three applied laser beams, spread out over the whole ensemble. A fourth laser beam is used for the readout. The qubits result from the interaction of the electron spin with a uniform magnetic field (B). The system is kept at a temperature around 7 K. Essential elements of the architecture considered here are schematically illustrated in Fig. 1, where

*Present address: Centro de Ciências Biológicas e da Natureza, Universidade Federal do Acre – Caixa Postal 500, Rio Branco, AC 69915-900, Brazil

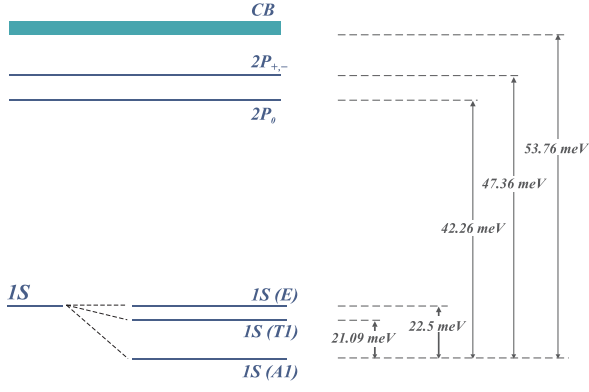


FIG. 2: **Orbital energy levels of As in Si.** Only the relevant levels are shown. Here CB stands for conduction band.

we represent an array of donors positioned at the maxima of the cavity mode. One- and two-qubit logical gates, as well as system initialization and readout, are implemented through the external laser beams, which address all qubits simultaneously. The coupling between a donor electron and the light fields may be interrupted by an external electric field, due to the Stark shift of the donor levels. This effect is explored for selecting the target qubits for one- or two-qubit operations. Two-qubit operations are mediated by the vacuum field of the photonic-crystal cavity [6].

The study of group-V donor impurities in silicon is a quite mature field [14, 15]. When a group-V element, such as P, As or Sb, substitutes the group-IV Si atom in bulk Si, an additional electron is incorporated in the system. This electron remains bound to the core potential via a screened Coulomb interaction, constituting a solid-state analogue of the hydrogen atom. Electronic-structure peculiarities of bulk silicon lead to a modified hydrogenic spectrum for the donor. Experimental values for the lowest energy levels and relative energies for As donors in silicon [15] are given in Fig. 2.

Qubit states are defined within the $1S(A1)$ (see Fig. 2) ground state under a magnetic field B satisfying $g_e \mu_B B \gg A$, where A is the hyperfine coupling constant, μ_B is the Bohr magneton and $g_e (\approx 2)$ is the electron Landé factor in Si. For As in Si, $A = 400$ MHz, so a magnetic field $B = 0.3$ T will decouple nuclear and electron spin states, generating well-defined electron spin states $|\downarrow\rangle$ and $|\uparrow\rangle$ as qubits, with a 10 GHz splitting.

One-qubit operations are implemented through Raman coupling of the states $|\downarrow\rangle$ and $|\uparrow\rangle$ of donors previously selected by switching off the Stark-shift electric fields acting on them. In this excitation scheme, the donors interact with two laser fields of Rabi frequencies Ω_{L1} and Ω_{L2} , and frequencies ω_{L1} and ω_{L2} , respectively, detuned from the transitions between the qubit states $|\downarrow\rangle$ and $|\uparrow\rangle$ and the states $|2P_{+,-}\rangle$ by Δ , as shown in Fig. 3(a) (the fine structure splitting of the levels $2P_{+,-}$ is not shown). If $\Delta \gg \Omega_{L1}, \Omega_{L2}, \Gamma_p$, with Γ_p being the decay rate of the levels $2P_{+,-}$, the levels $2P_{+,-}$ are only virtually populated, giving rise to an effective coupling between levels $|\downarrow\rangle$ and $|\uparrow\rangle$, described, in

the interaction picture, if $\Omega_{L1} = \Omega_{L2}$, by the Hamiltonian $\hat{H}_{\text{eff}} = \hbar \Omega_{\text{eff}} |\downarrow\rangle\langle\uparrow| + H.c.$, where $\Omega_{\text{eff}} = |\Omega_{L1}|^2 / \Delta$.

During the Raman coupling of the qubit states there is a small probability, of the order $\Omega_{\text{eff}} / \Delta$, of populating the intermediate level $2P_{+,-}$. This will lead to decoherence of the one-qubit operations with the rate $\Omega_{\text{eff}} (\Gamma_p / \Delta)$ due to the spontaneous decay of the level $2P_{+,-}$. Since the time required for one-qubit operations is of the order of $1 / \Omega_{\text{eff}}$, the error probability per gate will be $\epsilon_1 \approx \Gamma_p / \Delta$.

We propose a spin-orbit (SO) mediated coupling for the opposite-spin qubit states. In order to avoid destructive interference effects that would make Ω_{eff} vanishingly small, the intensity ζ of the SO coupling among the states within the $2P_{+,-}$ manifold must be comparable or larger than the detuning Δ of the laser fields. Strong SO splittings have been measured for states of the fundamental manifold in the group VI donors Se:Si and Te:Si, and of their corresponding ionized states [16, 17, 18]. For Se:Si, the measured SO coupling is 3.2 cm^{-1} (96 GHz); so we assume in our calculations for As, the element corresponding to the Se row in the periodic table, a coupling of the same order of magnitude, $\zeta \sim 100$ GHz.

The SO coupling also mediates an efficient mechanism for selectively turning on and off the interaction between the qubits and the light fields through an applied electric field produced by the electrode above each donor. The electric field has two effects: It increases the detuning between the Raman laser fields and the atomic transition, so that it becomes much higher than the SO splitting, and it mixes 2P and 2S states. The increase of the detuning causes a destructive interference between the 2P states, which leads to the vanishing of the Raman transition. The mixing of 2P and 2S states also reduces the Raman coupling, since the 2S state does not couple with the ground state. Perturbation theory indicates that the combined effect reduces the transition probability by a factor equal to the third power of the ratio between the SO coupling and the electric dipole energy, which leads to an error of the order of 10^{-4} for an applied field equal to 20 kV/cm. This field is below the ionization threshold for P in Si [19], and for As the threshold should be even higher since the binding energies are larger. Only the donors that are subjected to smaller electric fields will be affected by the Raman coupling. This scheme has the advantage that only quiescent atoms are subject to large electric fields, so that the essential properties of the active atoms remain unchanged.

One-qubit operations are implemented with a linearly-polarized beam along the direction of the magnetic field (same polarization as for the cavity mode) and a circularly right-polarized beam, as shown in Fig. 3(a). Due to selection rules, the cavity mode does not affect one-qubit operations.

Two-qubit operations involve the interaction of a previously Stark-shift-selected pair of qubits with an additional laser beam and with the cavity mode. The frequencies and polarizations of the laser and cavity fields are chosen in such a way that they nearly satisfy the conditions for Raman coupling of the qubit states $|\downarrow\rangle$ and $|\uparrow\rangle$ for each donor [6] (see Fig. 3(b)). The wavelength for the transition $1S(A1) \rightarrow 2P_{+,-}$ is 26.39 μm in vacuum; in Si (dielectric constant $\epsilon = 11.4$), the corresponding value is $\lambda = 7.82 \mu\text{m}$. The wavelengths of the

cavity mode and the laser beams should be around this value.

Under the conditions established for a Raman transition and in the dispersive regime, i.e., $\Delta_L^i \gg \Omega_L, \Gamma_p$ and $\Delta_C^i \gg \Omega_C, \Gamma_p, \Gamma_C$, where Ω_C quantifies the coupling with the cavity mode, with width Γ_C , the states $2P_{+,-}$ are only virtually occupied, giving rise to an effective coupling between the cavity mode and the qubit states which, in an adequate interaction picture, is described by the Hamiltonian:

$$\hat{H}_{\text{eff}} = \sum_i \left[\hbar \Omega_{\text{eff}}^i \hat{a} \hat{\sigma}_-^i e^{-i\delta^i t} + H.c. \right], \quad (1)$$

where \hat{a} is the annihilation operator for the cavity field, $\sigma_-^i = |\downarrow\rangle_i \langle \uparrow|_i$ is the spin flip operator for donor i , $\delta^i = \Delta_L^i - \Delta_C^i$, and the sum extends over all the donors selected by the electric static fields. The couplings Ω_{eff}^i are defined as:

$$\Omega_{\text{eff}}^i = \frac{1}{2} \Omega_L \Omega_C^* \left(\frac{1}{\Delta_L^i} + \frac{1}{\Delta_C^i} \right). \quad (2)$$

If $\delta_i \gg \Omega_{\text{eff}}^i, \Gamma_C$, the cavity field will be only virtually excited and can be eliminated from the dynamics, leading to an effective two-qubit interaction mediated by the vacuum of the cavity mode:

$$\hat{H}_{ij} = \sum_{i \neq j} \left[\hbar \Omega_{ij} \hat{\sigma}_+^i \hat{\sigma}_-^j e^{i\delta^{ij} t} + H.c. \right], \quad (3)$$

where $\delta^{ij} = \delta^i - \delta^j$. From Eq. (3), one can see that each pair of qubits i, j that satisfies $\delta^i = \delta^j$ will resonantly interact through the Hamiltonian

$$\hat{H}_{ij} = \hbar \Omega_{ij} \hat{\sigma}_+^i \hat{\sigma}_-^j + H.c., \quad (4)$$

with the effective coupling constant $\Omega_{ij} = \left[\Omega_{\text{eff}}^i \left(\Omega_{\text{eff}}^j \right)^* \right] / \delta^i$. The qubit pairs for which $\delta^{ij} \gg \Omega_{ij}$ will interact off-resonantly and will not couple to each other. The error probability per gate for two-qubit operations can be found in a similar way as for one-qubit operations and will be given by $\epsilon_2 \approx \Gamma_C / \delta^i$.

The Hamiltonian (4) implements the $\sqrt{\text{SWAP}}$ operation $|\uparrow\uparrow\rangle \rightarrow (|\uparrow\downarrow\rangle + |\downarrow\uparrow\rangle) / \sqrt{2}$, which, combined with single-qubit rotations, can be used to implement a CNOT gate [5].

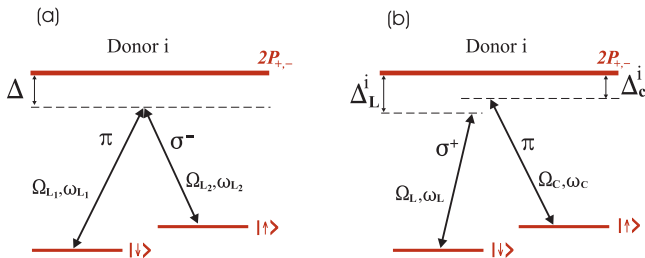


FIG. 3: **Logical gates.** (a) One-qubit operations are implemented with a linearly polarized beam along the direction of the magnetic field and a circularly right-polarized beam; (b) Two-qubit operations are implemented with a linearly polarized cavity field along the direction of the magnetic field and a circularly left-polarized laser beam.

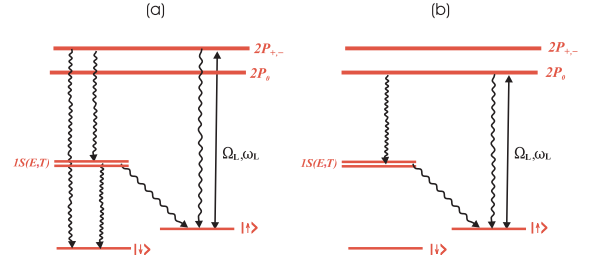


FIG. 4: **Initialization and readout.** (a) Initialization: population of qubit state $|\uparrow\rangle$ is transferred to the qubit state $|\downarrow\rangle$ via optical pumping by resonantly exciting transition $|\uparrow\rangle \leftrightarrow 2P_{+,-}$ with laser light; (b) Readout of the qubit-state is made by monitoring the fluorescence light of the cyclic transition $|\uparrow\rangle \leftrightarrow 2P_0$.

$\sqrt{\text{SWAP}}$ operations can be implemented in parallel, by having different pairs, with $\delta^i = \delta^j, \delta^k = \delta^l$, but $|\delta^i - \delta^k| \gg |\Omega_{ij}|$.

The qubits are initialized by driving resonantly the transition $|\uparrow\rangle \leftrightarrow 2P_{+,-}$ with a laser beam. Under the action of the magnetic field B and at temperatures of the order of 7 K only the state $1S(A1)$ will be populated. Since the level $2P_{+,-}$ is unstable, it will decay to one of the qubit levels, leading to optical pumping of the level $|\downarrow\rangle$ (see Fig. 4(a)).

Qubit readout takes advantage of the fact that the states of the $2P_0$ manifold do not show SO coupling. If laser light excites resonantly the transition $|\uparrow\rangle \leftrightarrow 2P_0$, only the states of that manifold with the same electronic spin as the state $|\uparrow\rangle$ are excited. Due to selection rules, the radiative- or phonon-assisted decay of these states to states with different electronic spin is forbidden. The decay out of the $2P_0$ level is radiative, whereas the decay out of level $1S(E)$ is phonon assisted. For this reason, all the excitation will decay back to the state $|\uparrow\rangle$. Therefore the transition $|\uparrow\rangle \leftrightarrow 2P_0$ is cyclic and the electron shelving technique can be used to measure the occupation of the qubit states [20]: If, during the laser excitation of the transition $|\uparrow\rangle \leftrightarrow 2P_0$ fluorescence light is observed, the qubit was in state $|\uparrow\rangle$, otherwise the state $|\downarrow\rangle$ was occupied (see Fig. 4(b)). Since the decay $1S(E) \rightarrow |\uparrow\rangle$ is assisted by acoustic phonons, part of the fluorescence light differs in frequency from the laser exciting the transition $|\uparrow\rangle \leftrightarrow 2P_0$, which implies that it is possible to distinguish the fluorescence signal from scattered laser radiation.

The feasibility of the proposed scheme is based on the following estimates for the frequencies, couplings, and times involved in the one-qubit, two-qubit and readout operations.

The measured absorption linewidth of the $1S(A1) \rightarrow 2P_{+,-}$ transition for Si:P is approximately 1GHz [21], giving an upper bound for the decay rate Γ_p . This rate could be strongly decreased (more than one order of magnitude), since phonon-mediated decay can be suppressed by applying stress, as demonstrated in Ref. [22], and spontaneous radiative transitions from these levels are also strongly suppressed due to the photonic band gap, since they are far detuned from the cavity mode of the photonic crystal [23]. The Raman-coupling conditions are satisfied, for example, for $\Omega_{L1}/2\pi = \Omega_{L2}/2\pi =$

2GHz and $\Delta = 200\text{GHz}$. This would lead to an effective Rabi frequency $\Omega_{\text{eff}}/2\pi = 20\text{MHz}$ and an error probability per gate $\epsilon_1 \approx 10^{-4}$. For these parameters, which correspond to laser powers of the order of 10 mW, the typical time for a one-qubit operation would be of the order of 50 ns, much shorter than a spin decoherence time of 60 ms. Under the same conditions, we have calculated that the error probability per gate induced by eventual impurity ionization, due to two-photon absorption, is negligibly small ($\epsilon \approx 6 \times 10^{-7}$).

For the two-qubit operations, one could choose, for example, $\Omega_C^i/2\pi \sim 30\text{MHz}$ (this value corresponds to a modal volume $100\lambda^3$), $\Omega_L^i/2\pi \sim 5\text{GHz}$, $\Delta_L^i = 100\text{GHz}$ and $\Delta_C^i = 99\text{GHz}$. This yields an effective two-qubit coupling $\Omega_{ij}/2\pi \sim 2.25\text{KHz}$, which allows one to perform more than $10^3 \sqrt{\text{SWAP}}$ operations within a qubit decoherence time of 60 ms. Since for two-qubit operations the error per gate is $\epsilon_2 \approx \Gamma_C/\delta_i$, an error per gate of the order of 1×10^{-3} would imply a cavity decay rate $\Gamma_C \approx 1\text{MHz}$. This requires a cavity quality factor $Q \approx 10^7$. Quality factors of 10^6 have already been reported for silicon-based photonic-crystal nanocavities [13]; Q 's as high as 2×10^7 seem to be within reach [13]. Larger wavelengths in the μm region, as used in our proposal, should lead to yet higher values of Q . Combined with larger values of the spin decoherence time, consistent with the experimental results [10, 24], this would allow one to increase δ , further reducing the error per gate.

Readout is very fast, since the decay rate out of level P_0 is of the order of 1 GHz whereas the phonon-assisted decay of level $1S(E)$ is of the order of 10^{-10} s [25]. We estimate that about 10000 cycles, corresponding to a detection time around 1 μs , should yield a reading efficiency close to 100%. Parallel readout can be implemented for donors separated by ten cavity wavelengths or more.

Finally, we address a crucial fabrication issue: Given that the best currently achievable deposition control for impuri-

ties in Si is $\sim 10 \text{ \AA}$ [26], the impact of small donor misplacements on the proposed device operation must be analyzed. A deviation $\delta\vec{r}$ in the position of a donor from a maximum of the cavity field (see Fig. 1) introduces a variation $\Delta\Omega_C \approx 2\pi^2(|\delta\vec{r}|/\lambda)^2\Omega_C$ on the cavity vacuum Rabi frequency Ω_C at the position of the donor. Here $\lambda = 7.8 \mu\text{m}$ is the cavity wavelength. This implies that $|\delta\vec{r}| = 100\text{\AA}$ leads to $\Delta\Omega_C \approx 3 \times 10^{-5}\Omega_C$. The time for a typical two-qubit gate such as $\sqrt{\text{SWAP}}$ is $t \sim 1/\Omega_{ij}$, leading to an error probability in this operation of $p \approx (\Delta\Omega_C/\Omega_C)^2 \approx 1 \times 10^{-9}$, which means that our operation scheme is quite insensitive to relatively large (several lattice parameters) donor misplacement within the simple donor linear array architecture. This is in contrast with Kane's original exchange-based proposal, which leads to much more stringent conditions on impurity positioning, and requires elaborate two-dimensional architectures to compensate for donor misplacement [27].

Our estimations indicate that the present proposal could meet the conditions for a robust quantum computation device. The precise quantum control of atoms and ions in optical cavities, already demonstrated in several labs, and the fact that Si is the leading material in terms of processing and device fabrication, with sophisticated techniques for impurity implantation and high- Q microcavity construction, indicate that this system might be a viable candidate for a working quantum computer using achievable technological resources.

Acknowledgments

The authors acknowledge financial support from the Brazilian funding agencies CNPq, CAPES, PRONEX, FUJB and FAPERJ. This work was performed as part of the Brazilian Millennium Institutes for Quantum Information and Nanotechnology.

-
- [1] M. Nielsen & I. Chuang, *Quantum Computation and Quantum Information* (Cambridge Univ. Press, Cambridge, UK, 2000).
 - [2] P. Aliferis and A. W. Cross, *Phys. Rev. Lett.* **98**, 220502 (2007).
 - [3] E. Knill, *Nature* **434**, 39 (2005).
 - [4] P. Aliferis, D. Gottesman, and J. Preskill, *Quant. Inf. Comput.* **8**, 181(2008).
 - [5] D. Loss and D. P. DiVincenzo, *Phys. Rev. A* **57**, 120 (1998).
 - [6] A. Imamoglu *et al.*, *Phys. Rev. Lett.* **83**, 4204 (1999).
 - [7] B. E. Kane, *Nature* **393**, 133 (1998).
 - [8] B. E. Kane, *MRS BULLETIN* **30**, 105 (2005).
 - [9] J. R. Petta *et al.*, *Science* **309**, 2180 (2005).
 - [10] A. M. Tyryshkin *et al.*, *Phys. Rev. B* **68**, 193207 (2003).
 - [11] N. Isailovic *et al.*, *ACM Transactions on Architecture and Code Optimization*. **1**, 34 (2004).
 - [12] B. Koiller, X. D. Hu, and S. Das Sarma, *Phys. Rev. Lett.* **88**, 027903 (2002).
 - [13] B. -S. Song *et al.*, *Nature Materials* **4**, 207 (2005).
 - [14] W. Kohn, *Solid State Physics* Vol. 5 (eds Seits, F. & Turnbull, D.) 257 (Academic, New York, 1957).
 - [15] A. K. Ramdas and S. Rodriguez, *Rep. Prog. Phys.* **44**, 1297 (1981).
 - [16] K. Bergman *et al.*, *Phys. Rev. Lett.* **56**, 2827 (1986).
 - [17] H. G. Grimmeiss, E. Janzén, and K. Larsson, *Phys. Rev. B* **25**, 2627 (1982).
 - [18] R. E. Peale *et al.*, *Phys. Rev. B* **18**, 10829 (1988).
 - [19] A. Debernardi, A. Baldereschi, and M. Fanciulli, *Phys. Rev. B* **74**, 035202 (2006).
 - [20] D. Leibfried *et al.*, *Rev. Mod. Phys.* **75**, 281 (2003).
 - [21] D. Karaiskaj *et al.*, *Phys. Rev. Lett.* **90**, 186402 (2003).
 - [22] S. G. Pavlov *et al.*, *Appl. Phys. Lett.* **90**, 141109 (2007).
 - [23] K. Hennessy *et al.*, *Nature* **445**, 896 (2007).
 - [24] S. Das Sarma *et al.*, *Solid State Comm.* **133**, 737 (2005).
 - [25] S. G. Pavlov *et al.*, *Phys. Rev. Lett.* **84**, 5220 (2000).
 - [26] S. R. Schofield *et al.*, *Phys. Rev. Lett.* **91**, 136104 (2003).
 - [27] L. C. L. Hollenberg *et al.*, *Phys. Rev. B* **74**, 045311 (2006).